



Alexandria University
Alexandria Engineering Journal

www.elsevier.com/locate/aej
www.sciencedirect.com



ORIGINAL ARTICLE

Mathematical modeling of entropy generation in magnetized micropolar flow between co-rotating cylinders with internal heat generation



Srinivas Jangili ^{a,*}, Nagaraju Gajjela ^b, O. Anwar Bég ^c

^a Department of Mathematics, National Institute of Technology, Meghalaya, Shillong 793003, India

^b Department of Mathematics, GITAM University, Hyderabad Campus, Telangana 502329, India

^c Fluid Mechanics, Spray Research Group, Room G77, Newton Building, School of Computing, Science and Engineering (CSE), University of Salford, M54WT, UK

Received 20 May 2016; revised 14 July 2016; accepted 19 July 2016

Available online 1 August 2016

KEYWORDS

MHD flow;
Micropolar fluid;
Entropy generation analysis;
Convective cooling;
Heat generation

Abstract The present study investigates the entropy generation in magnetized-micropolar fluid flow in between two vertical concentric rotating cylinders of infinite length. The surface of the inner cylinder is heated while the surface of the outer cylinder is cooled. Internal heat generation is incorporated. The Eringen thermo-micropolar fluid model is used to simulate the micro-structural rheological flow characteristics in the annulus region. The flow is subjected to a constant, static, axial magnetic field. The surface of the inner cylinder is prescribed to be isothermal whereas the surface of the outer cylinder was exposed to convection cooling. The conservation equations are normalized and closed-form solutions are obtained for the velocity, microrotation, temperature, entropy generation number, Bejan number and total entropy generation rate. The effects of the relevant parameters are displayed graphically. It is observed that the external magnetic force enhances the entropy production rate and it is maximum in the proximity of the inner cylinder. This causes more wear and tear at the surface of the inner cylinder. Greater Hartmann number also elevates microrotation values in the entire annulus region. The study is relevant to optimization of chemical engineering processes, nuclear engineering cooling systems and propulsion systems utilizing non-Newtonian fluids and magnetohydrodynamics.

© 2016 Faculty of Engineering, Alexandria University. Production and hosting by Elsevier B.V. This is an open access article under the CC BY-NC-ND license (<http://creativecommons.org/licenses/by-nc-nd/4.0/>).

1. Introduction

Mathematical modeling of fluid flow in a gap between two concentric vertical/horizontal rotating cylinders is very important due to considerable applications in diverse arrays of engineering technologies, including journal porous bearings, commercial viscometers, swirl nozzles, and electrical motors

* Corresponding author.

E-mail addresses: j.srinivasnit@gmail.com (S. Jangili), naganitw@gmail.com (N. Gajjela), o.a.beg@salford.ac.uk (O. Anwar Bég).

Peer review under responsibility of Faculty of Engineering, Alexandria University.

<http://dx.doi.org/10.1016/j.aej.2016.07.020>

1110-0168 © 2016 Faculty of Engineering, Alexandria University. Production and hosting by Elsevier B.V.

This is an open access article under the CC BY-NC-ND license (<http://creativecommons.org/licenses/by-nc-nd/4.0/>).

(Maron and Cohen [1]). Couette [2] was the first to study the problem of flow between two rotating cylinders for Newtonian fluids. Besides this, the analysis of heat transfer in an annulus, where the inner/outer cylinder rotates (or one cylinder rotates or both cylinders are stationary), is an important research area in many scientific applications related to engineering and science, such as in transport of petroleum and water, food processing, chemical systems and the automobile industry. Representative studies of annular flows in the context of journal bearings have been communicated by Pillai and Varma [3], Bujurke and Naduvinamani [4], Lin [5] and Ruggiero et al. [6]. A porous journal bearing has been proposed to improve the performance of solid journal bearings. Schlichting [7] discussed the velocity and temperature distributions in the case of Couette flow. Many other theoretical studies have been reported in recent years. Channabasappa and colleagues [8] investigated the effect of the porous lining thickness on velocity distributions and wall shear stresses at the inner and outer cylinder walls. They showed that the presence of porous lining enhances the shear stress. Bathaiah and Venugopal [9] examined the flow between two concentric circular cylinders by considering the presence of a uniform magnetic field in the annulus region. They noticed that the temperature of the fluid increases in the proximity of the inner cylinder, whereas the opposite behavior is observed at the outer cylinder. Lee [10] experimented to find out the rotational effects on the low Prandtl number fluid flows between the regions of eccentric and concentric cylinders. His results showed that the increase in the Rayleigh number increases the average Nusselt number for both the cases of eccentric and concentric rotating cylinders. Batra and Das [11] considered the flow of a Casson fluid in an annulus region between two rotating cylinders where the outer cylinder is adjacent to a porous lining material. In another work, Batra and Eissa [12] obtained computational solutions for laminar flow of Sutterby rheological fluid in between two cylinders using a finite difference method. Leong and Lai [13] derived perturbation expansion analytical solutions for flow and heat transfer characteristics of flow in between two cylinders where the outer cylinder is lined with a porous material. Ravanchi et al. [14] investigated analytically viscoelastic flow in between two concentric cylinders where the outer cylinder is at rest, using the Giesekus model. They observed that an increase in the Weissenberg number enhances the velocity gradient near the inner cylinder. Subotic and Lai [15] analyzed the fluid flow and heat transfer characteristics in an annulus region between two rotating cylinders where the porous layer is attached to surface of the outer cylinder. Barletta et al. [16] analyzed the mixed convection flow in a region between two cylinders filled with a porous medium. Mahmood et al. [17] presented closed-form expressions for shear stress and the velocity profile for the flow of a generalized Maxwell fluid between two infinite coaxial circular cylinders. Recently, Mozayyeni and Rahimi [18] obtained a numerical solution for mixed convection flow of a viscous fluid in an annulus of horizontal concentric cylinders with different uniform wall temperatures in both steady and unsteady states using finite volume method.

In the past few decades, the thermal efficiency of a system has been determined generally using the First Law of Thermodynamics (FLT). In recent years, however, researchers have identified that entropy generation analysis via the Second Law of Thermodynamics (SLT) is more appropriate and accu-

rate than via the first law of thermodynamics. It is well known that most thermal processes are inherently irreversible. The irreversibility in a system manifests in a continuous entropy generation, which destroys the exergy (useful energy or available energy for work) of a system. This exergy loss is mainly generated by heat transfer which occurs in different modes i.e., conduction, convection and radiation, which are very common in most thermal engineering systems. Besides these, additional effects including fluid friction (viscosity), buoyancy and magnetic field may also contribute to this entropy production. The loss of exergy in any thermal equipment should be minimized to achieve an optimal usage of the energy situation with minimum irreversibilities. This optimum condition can be assessed via entropy generation minimization (EGM). A detailed discussion on entropy generation analysis for a diverse range of flow systems was first presented by Bejan [19]. A number of works on entropy generation analysis for various flow configurations have been emerged in the literature. In the present work we are more concerned with analytical/numerical studies related to entropy generation in between two concentric rotating cylinders. Yilbas [20] studied the entropy generation for an incompressible Newtonian fluid in an annulus of two cylinders with the outer cylinder rotating and the inner cylinder stagnant, noting that the minimum entropy production occurs when the temperature is maximized. Mahmud and Fraser [21] examined the entropy generation characteristics of a viscous fluid between two cylinders, observing that both the cylinders act as strong concentrators of heat transfer irreversibility. Mahmud and Fraser [22] further discussed the heat transfer characteristics in an annulus region between two cylinders, highlighting that the entropy is maximum due to the larger velocity and temperature gradients occurring near the inner cylinder. Mirzazadeh et al. [23] investigated the thermodynamic characteristics for viscoelastic fluid flow in the annular space between two cylinders subjected to different boundary conditions, identifying that the irreversibility in the annulus increases with a rise in Brinkman number. Hamakawa et al. [24] performed an experimental study of fluid flow between two concentrating cylinders with cavities where the inner cylinder is rotating and the outer cylinder is at rest. Tshella and Makinde [25] examined the effect of variable viscosity flow on entropy between two concentric pipes at rest with convective cooling imposed at the outer cylinder. They observed that the inner pipe surface produces greater entropy owing to high temperature gradients.

Many classical fluid flow problems have been extended to include magnetohydrodynamic (MHD) effects where the fluid is electrically-conducting and responds to a magnetic field. Globe [26] was the first author who had shown interest to study the rotation of magnetohydrodynamic flow in an annular space between two cylinders. In recent years, the study of magnetohydrodynamic flows and their influence on the entropy generation in thermal processes has acquired a great attention owing to ever-growing applications in industry, particularly in cooling of nuclear reactors, MHD micropumps, microelectronic devices, MHD marine propulsion and in particular MHD energy systems in which exergy analysis has been applied extensively [27–31]. A major motivation in this last area (energy systems) is the ever-growing need to minimize power losses and increase the economic viability of alternate energy systems. Fundamental work in magnetohydrodynamic flow between rotating cylinders includes Mahian et al. [32]

who studied the magnetohydrodynamic flow of Newtonian viscous fluid in between two rotating cylinders. They noticed that with an increase in magnetic field, entropy production in the proximity of the inner cylinder is reduced, whereas in the annulus region it is increased. Mahian et al. [33] also investigated the entropy effects on magnetohydrodynamic flow between two isothermal cylinders. They have constructed the distributions for entropy generation and Bejan number and observed that a decrease in the radius ratio results in a depletion in the entropy generation rate. In the other work, Mahian et al. [34] further applied second law analysis to analyze the entropy characteristics of TiO₂-water magnetic nanofluid flow between two rotating cylinders, showing that an increase in magnetic parameter results in a strong elevation in the average entropy generation number. Interested readers will find studies in [35–43] and references therein very useful.

In the last five decades, the research towards non-Newtonian transport phenomena has significantly been increased due to continuously emerging applications in various industrial systems. Many non-Newtonian working fluids possess intricate microstructure. Eringen developed the micropolar fluid theory [44] in 1966 as a simplification of his earlier general micro-morphic (“simple microfluid”) theory [45,46] to simulate complex features of real non-Newtonian fluids in which fluid micro-elements can sustain gyratory motions, couple stresses, body couples and possesses a non-symmetric stress tensor. In addition to the usual velocity vector, the fluid particles in micropolar theory have an independent kinematic (rotation vector) known as the microrotation (angular velocity) vector. This theory has provided a good model for studying a number of very sophisticated industrial fluids, e.g. polymers, suspension fluids, paints, liquid crystals, colloidal solutions, lubricating oils, fluids with additives, physiological and environmental liquids. For details of the theory of micropolar fluid and its applications, the reader may refer to the books by Stokes [47] and Lukaszewicz [48]. Although Reiner [49] performed the first investigation into non-Newtonian flow between two cylinders, micropolar studies were reported much later. Ariman et al. [50] considered the Couette and Poiseuille flows for micropolar fluid between two coaxial cylinders. Ramkissoon and Majumdar [51] discussed the flow of a micropolar fluid between two concentric cylinders in the case where the inner cylinder is subjected to an arbitrary time-dependent angular velocity whereas the outer cylinder is stationary. They employed integral transforms to obtain exact solutions and observed that micropolar fluids generate greater couple on the inner cylinder relative to Newtonian fluids.

On the other hand, a large number of articles have appeared focusing on the analysis of entropy generation for the case of Newtonian viscous fluids. For example, Kamisli [52] studied theoretically the entropy generation in the steady flow of Newtonian viscous fluid in a thin horizontal channel also considering the wall mass flux (suction and injection) effects. Mahmud and Fraser [53] applied the thermodynamic second law to eight different types of geometries under various boundary conditions for both Newtonian and non-Newtonian fluids. However, relatively very few researchers have analyzed the entropy generation characteristics of micropolar fluids. Of the few studies communicated, we mention Srinivasacharya and Hima Bindu [54] studied the entropy generation of micropolar fluid flow in a gap between two infinite vertical concentric cylinders. Very recently, Ramana Murthy and

Srinivas [55] examined entropy generation in the flow of two immiscible micropolar fluids in a horizontal channel.

The principal objective of the current work is to investigate analytically the entropy generation in magnetohydrodynamic flow of an electrically-conducting thermo-micropolar fluid inside the annulus region of two rotating cylinders. The organization of the problem is as follows: In Section 2, the geometry of the problem is explained and then the governing equations of the problem are reduced to non-dimensional form and solved to give exact analytical solutions. Next the fluid flow and heat transfer aspects of the problem are addressed to derive velocity, microrotation and temperature distributions obtained in this section. Subsequently, in Section 3, the dimensionless expression for the entropy generation number, Bejan number and total entropy generation number are given via the second law of thermodynamics. The influence of various thermo-physical and rheological flow parameters on velocity, microrotation, temperature, entropy generation number, Bejan number and total entropy generation number is elucidated graphically and interpreted in detail. Finally, in Section 4 the major conclusions of the present analysis are summarized and future pathways for research in this area are identified.

2. Mathematical formulation

The physical regime under investigation comprises steady, incompressible, laminar micropolar fluid flow between two co-rotating cylinders of radii a and b , respectively. It is assumed that the outer cylinder wall thickness is negligible and has the same thermal conductivity as that of the fluid. The inner and the outer cylinders are rotating in anti-clockwise direction at different angular velocities ω_1 and ω_2 , respectively (see Fig. 1).

A uniform static external magnetic field B_0 is applied in the axial direction. The fluid motion is rotationally symmetric, the axial velocity W is zero and there is no flow along the radial direction (U is absent), and also the derivatives of V (transverse velocity) with respect to θ and z vanish. Intrinsic to the present study is that the magnetic Reynolds number is assumed to be very small (due to small electric conductivity), so that the induced magnetic field can be omitted in comparison with the applied external magnetic field. In such a scenario, the advection will be dominated by diffusion. Furthermore, the strength of the magnetic field is insufficient to generate Hall currents. The inner cylinder fluid surface is kept at temperature T_1 while the outer cylinder surface is subjected to convection by a coolant at temperature T_∞ . In the present problem, the fluid thermal properties are temperature-independent.

Under the above assumptions (buoyancy force is neglected), the governing equations for incompressible magnetized micropolar fluid [44–46] flow in the annular region are as follows:

$$\frac{dP}{dR} = \rho \frac{V^2}{R} \quad (1)$$

$$-\kappa \frac{dC_1}{dR} + (\mu + \kappa)D^2V - \sigma B_0^2V = 0 \quad (2)$$

$$-2\kappa C_1 + \kappa \left(\frac{dV}{dR} + \frac{V}{R} \right) + \gamma \left(\frac{d^2C_1}{dR^2} + \frac{1}{R} \frac{dC_1}{dR} \right) = 0 \quad (3)$$

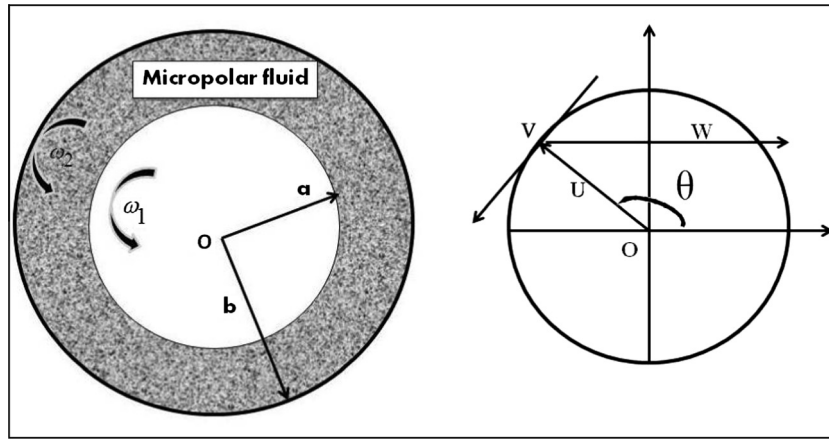


Figure 1 Schematic diagram of concentric rotating annuli.

$$\begin{aligned} &K \left(\frac{d^2 T}{dR^2} + \frac{1}{R} \frac{dT}{dR} \right) + \mu \left(\frac{dV}{dR} - \frac{V}{R} \right)^2 + 4\kappa \left(\frac{1}{2} \left(\frac{dV}{dR} + \frac{V}{R} \right) - C_1 \right)^2 \\ &+ \beta \left(\frac{dC_1}{dR} \right)^2 + \dot{q} = 0 \end{aligned} \tag{4}$$

where $D^2 = \frac{d^2}{dR^2} + \frac{1}{R} \frac{d}{dR} - \frac{1}{R^2}$.

The scalar quantities ρ and σ are, respectively, the density and electrical conductivity and are assumed to be constants. Here V is the tangential velocity, C_1 is microrotation in axial direction, T is the fluid temperature, \dot{q} is the internal heat generation and P is the fluid pressure at any point. The material constants (μ, κ) designate the viscosity coefficients (Newtonian dynamic viscosity and Eringen vortex viscosity, respectively), (β, γ) are gyro-viscosity coefficients, and K is the thermal conductivity. Two sets of boundary conditions are imposed, as follows:

The boundary conditions for inner and outer cylinders are as follows:

- (i) $V = a\omega_1$ at $R = a$ (no-slip condition)
- (ii) $C_1 = \omega_1$ at $R = a$ (hyper-stick condition)
- (iii) $T = T_1$ at $R = a$ (isothermal condition at inner cylinder)
- (iv) $V = a\omega_2$ at $R = b$ (no-slip condition)
- (v) $C_1 = \omega_2$ at $R = b$ (hyper-stick condition)
- (vi) $-K \left(\frac{dT}{dr} \right)_{r=b} = \alpha [T(R=b) - T_\infty]$ (convective boundary condition at the outer surface) where α is the convective heat transfer coefficient.

The following non-dimensional quantities are deployed to obtain the dimensionless form of the governing equations and the associated boundary conditions:

$$\begin{aligned} V &= va\omega_1, \quad R = ra, \quad C_1 = C\omega_1, \quad P = p\rho a^2 \omega_1^2, \\ T &= \theta(T_1 - T_\infty) + T_\infty, \quad r_0 = \frac{b}{a}, \quad n = \frac{\omega_2}{\omega_1}, \quad n_1 = nr_0 \end{aligned} \tag{5}$$

In view of Eq. (5), the conservation Eqs. (1)–(4) assume the non-dimensional form:

$$\frac{dp}{dr} = \frac{v^2}{r} \tag{6}$$

$$-c \frac{dC}{dr} + D^2 v - M^2 v = 0 \tag{7}$$

$$-2sC + s \left(\frac{dv}{dr} + \frac{v}{r} \right) + \left(\frac{d^2 C}{dr^2} + \frac{1}{r} \frac{dC}{dr} \right) = 0 \tag{8}$$

$$\begin{aligned} \frac{d^2 \theta}{dr^2} + \frac{1}{r} \frac{d\theta}{dr} &= -Q - Br \left[\left(\frac{dv}{dr} - \frac{v}{r} \right)^2 \right. \\ &\left. + \frac{4c}{1-c} \left(\frac{1}{2} \left(\frac{dv}{dr} + \frac{v}{r} \right) - C \right)^2 + \delta \left(\frac{dC}{dr} \right)^2 \right] \end{aligned} \tag{9}$$

where $c = \frac{\kappa}{\kappa + \mu}$ is the coupling number or cross viscosity parameter ($0 \leq c < 1$), $M^2 = \frac{\sigma B_0^2 a^2}{\kappa + \mu}$ is the modified Hartmann number or magnetic body force parameter, $s = \frac{\kappa a^2}{\gamma}$ is the couple stress parameter, $Q = \frac{\dot{q} a^2}{K(T_1 - T_\infty)}$ is heat generation parameter, $Br = \frac{\mu a^2 \omega_1^2}{K(T_1 - T_\infty)}$ is the Brinkman number and $\delta = \frac{\beta}{\mu a^2}$ is another rheological parameter.

The associated boundary conditions in the non-dimensional form are as follows:

$$(i) v = 1, \quad (ii) C = 1, \quad (iii) \theta = 1 \text{ at } r = 1 \tag{10a}$$

$$(iv) v = n_1, \quad (v) C = n, \quad (vi) \frac{d\theta}{dr} = -\frac{Bi}{r_0} \theta \text{ at } r = r_0 \tag{10b}$$

where $Bi = \frac{\alpha a}{K}$ is the Biot number which essentially quantifies the relative significance of thermal (heat transfer) resistances within and at the surface of a body.

Eliminating $\frac{dC}{dr}$ from Eqs. (7) and (8), we arrive at the following equation for v :

$$D^4 v - (M^2 + (2-c)s)D^2 v + 2sM^2 v = 0 \tag{11}$$

The above equation can be expressed as follows:

$$(D^2 - \lambda_1^2)(D^2 - \lambda_2^2)v = 0$$

where $\lambda_1^2 + \lambda_2^2 = M^2 + s(2-c)$ and $\lambda_1^2 \lambda_2^2 = 2sM^2$. Since velocity v is finite in the interval $1 < r < r_0$, the solution of Eq. (11) can be written as follows:

$$v = a_1 I_1(\lambda_1 r) + a_2 K_1(\lambda_1 r) + a_3 I_1(\lambda_2 r) + a_4 K_1(\lambda_2 r) \tag{12}$$

The constants a_1, a_2, a_3, a_4 can be found by using the no slip boundary conditions on azimuthal velocity v and hyper-stick boundary conditions on microrotation C (from Eqs. (10a) and (10b)) and emerge as

$$\left. \begin{aligned} a_1 I_1(\lambda_1) + a_2 K_1(\lambda_1) + a_3 I_1(\lambda_2) + a_4 K_1(\lambda_2) &= 1 \\ a_1 I_1(r_0 \lambda_1) + a_2 K_1(r_0 \lambda_1) + a_3 I_1(r_0 \lambda_2) + a_4 K_1(r_0 \lambda_2) &= n_1 \\ a_1 \Delta_1 + a_2 \Delta_2 + a_3 \Delta_3 + a_4 \Delta_4 &= 2sc \\ a_1 \Delta_5 + a_2 \Delta_6 + a_3 \Delta_7 + a_4 \Delta_8 &= 2scn \end{aligned} \right\} \quad (13)$$

where

$$\begin{aligned} \Delta_1 &= (sc + \lambda_1^2 - M^2)(2I_1(\lambda_1) + \lambda_1 I_2(\lambda_1)); \\ \Delta_2 &= (sc + \lambda_1^2 - M^2)(2K_1(\lambda_1) - \lambda_1 K_2(\lambda_1)) \\ \Delta_3 &= (sc + \lambda_2^2 - M^2)(2I_1(\lambda_2) + \lambda_2 I_2(\lambda_2)); \\ \Delta_4 &= (sc + \lambda_2^2 - M^2)(2K_1(\lambda_2) - \lambda_2 K_2(\lambda_2)) \\ \Delta_5 &= (sc + \lambda_1^2 - M^2) \left(\frac{2I_1(r_0 \lambda_1)}{r_0} + \lambda_1 I_2(r_0 \lambda_1) \right); \\ \Delta_6 &= (sc + \lambda_1^2 - M^2) \left(\frac{2K_1(r_0 \lambda_1)}{r_0} - \lambda_1 K_2(r_0 \lambda_1) \right) \\ \Delta_7 &= (sc + \lambda_2^2 - M^2) \left(\frac{2I_1(r_0 \lambda_2)}{r_0} + \lambda_2 I_2(r_0 \lambda_2) \right); \\ \Delta_8 &= (sc + \lambda_2^2 - M^2) \left(\frac{2K_1(r_0 \lambda_2)}{r_0} - \lambda_2 K_2(r_0 \lambda_2) \right) \end{aligned} \quad (14)$$

Eq. (12) is solved for the velocities v and C using the boundary conditions (13).

The skin friction coefficient (C_f) at inner and outer cylinder surfaces in non-dimensional form is given by

$$C_f = \frac{2\overline{T}_{12}}{Re} \quad \text{at } r = 1 \text{ and } r = r_0 \quad (15)$$

where $\overline{T}_{12} = \frac{dv}{dr} - (1-c)\frac{v}{r} - cC$ and $Re = \frac{\rho a^2 \omega_1}{\mu + \kappa}$ is a modified Reynolds number.

3. Entropy generation analysis

The volumetric rate of entropy generation for magnetized-micropolar fluid is given as

$$\begin{aligned} S_G &= \frac{K}{T^2} \left(\frac{T_1 - T_\infty}{a} \right)^2 \left(\frac{d\theta}{dR} \right)^2 \\ &+ \frac{\omega_1^2}{T} \left[\mu \left(\frac{dV}{dR} - \frac{V}{R} \right)^2 + 4\kappa \left(\frac{1}{2} \left(\frac{dV}{dR} + \frac{V}{R} \right) - C_1 \right)^2 + \beta \left(\frac{dC_1}{dR} \right)^2 \right] \\ &+ \frac{1}{T} \sigma a^2 B_0^2 \omega_1^2 V^2 \end{aligned} \quad (16)$$

Using the aforementioned non-dimensional quantities, the equation for an entropy generation number N_S is defined as

$$\begin{aligned} N_S &= \frac{a^2 S_G}{K} = \frac{1}{\left(\theta + \frac{T_0}{1-T_0} \right)^2} \left(\frac{d\theta}{dr} \right)^2 \\ &+ \frac{Br}{\left(\theta + \frac{T_0}{1-T_0} \right)} \left[\left(\frac{dv}{dr} - \frac{v}{r} \right)^2 + \frac{4c}{1-c} \left(\frac{1}{2} \left(\frac{dv}{dr} + \frac{v}{r} \right) - C \right)^2 + \delta \left(\frac{dC}{dr} \right)^2 \right] \\ &+ \frac{M^2 Br}{1-c} \frac{1}{\left(\theta + \frac{T_0}{1-T_0} \right)} v^2 = N_H + N_F + N_M \end{aligned} \quad (17)$$

where $T_0 = \frac{T_\infty}{T_1}$ is the temperature ratio of the coolant fluid to the inner cylinder surface temperature. The first term ($= N_H$) on the right hand side of the Eq. (17) is the entropy due to heat transfer irreversibility, the second term ($= N_F$) is the entropy

due to fluid friction (viscous dissipation) and the third term ($= N_M$) is the entropy due to the magnetic force.

The total entropy generation number is therefore expressed as

$$S'_G = \int_A S_G L dA \quad (18)$$

where A is the cross-sectional area of the annulus space between two cylinders and L is the length of the rotating cylinders. Using the aforesaid non-dimensional quantities, the dimensionless total entropy generation rate (Nt) becomes

$$Nt = \frac{S'_G}{2\pi K L} = \int_1^{r_0} r N_S dr \quad (19)$$

In many engineering applications and entropy generation minimization studies, the contribution of heat transfer (N_H) and viscous dissipation (N_F) with magnetic force (N_M) to overall entropy generation rate (N_S) is required, since this provides a deeper insight into thermal optimization. In order to calculate irreversibility distribution, the Bejan number (Be) is introduced, which is the ratio of irreversibility due to heat transfer to the overall irreversibility due to heat transfer, fluid friction and magnetic effect.

$$Be = \frac{N_H}{N_H + N_F + N_M} \quad (20)$$

Generally Bejan number varies from 0 to 1. Accordingly, $Be = 0$ indicates that the irreversibility due to fluid friction and magnetic field is dominant whereas $Be = 1$ implies that the irreversibility due to heat transfer dominates. It is clear that when $Be = 0.5$, the irreversibility due to heat transfer by conduction is equal to the sum of the irreversibilities due to fluid friction and magnetic field.

4. Validation, results and discussion

An analytical model of magnetohydrodynamic flow of a micropolar fluid with internal heat generation between two concentric rotating cylinders has been developed. The boundary value problem has been solved subject to physically realistic boundary conditions to yield closed-form non-dimensional expressions for velocity, microrotation, temperature, entropy generation number, Bejan number and total entropy generation rate. To validate our solutions, we have compared with

Table 1 Comparison of the results of the velocity calculation of the present method and that of analytical solution [63] for a special case when $c = 0$.

r	Analytical solution (Assad and Oztop [63])	Present solution
1.0	1.0	1.02
1.2	1.17421	1.17422
1.4	1.35351	1.353512
1.6	1.53673	1.536732
1.8	1.72333	1.723333
2	1.91307	1.91307
2.2	2.10588	2.10589
2.4	2.30179	2.301792
2.6	2.50092	2.50093
2.8	2.70341	2.70339
3	2.90943	2.90942

earlier solutions of Assad and Oztop [63], for $c = 0$, documented in Table 1. The correlation is very close and therefore confidence in the present solutions is justifiably high. Here we describe results which have been numerically computed and presented graphically for diverse values of the couple stress parameter (s), coupling number (or micropolarity parameter) (c), Hartmann number (M), Brinkman number (Br), Biot number (Bi), internal heat generation parameter (Q) and temperature ratio (T_0).

Figs. 2a–2e display the influence of couple stress parameter (s) on velocity, microrotation, temperature, entropy generation number and Bejan number. From Fig. 2a, it is pointed out that there is a small decrease in the velocity profiles with greater couple stress parameter. From Figs. 2b and 2c, it is evident that with greater couple stress parameter (s), the microrotation profiles initially decreased in magnitude for lower radial coordinate values and thereafter are enhanced in magnitude with larger radius values. This implies that near the inner cylinder wall ($r = 1$) angular velocity of micro-elements is suppressed with greater couple stress effect, whereas the converse behavior is induced towards the outer wall ($r = 4$) of the annular gap. The effect is related to the space available to micro-elements for rotation. With greater progression into the gap annular region, the micro-elements are less constrained in their gyratory motions which serve to accelerate the micro-rotation, whereas closer to the inner cylinder wall, they are more restricted and this leads to angular velocity (micro-rotation) deceleration. However, there is never reverse spin induced since the magnitudes at all locations in the annular gap are sustained as positive. The temperature distributions, however respond in a very different manner to an increase in couple stress parameter (s), as observed in Fig. 2c – the profiles are monotonous ascents, and significantly different to the alternating behavior in the micro-rotation profiles, over the same incremental change in couple stress parameter. There is a steady growth in temperature magnitude from the inner wall of the annulus gap to the outer wall of the gap. Peak temperature is attained at $r \sim 2.5$ and thereafter a decrease is observed. Maximum temperature, therefore arises within the gap, not at the boundaries. Increasing couple stress parameter consistently decreases temperatures and manifests in a cooling

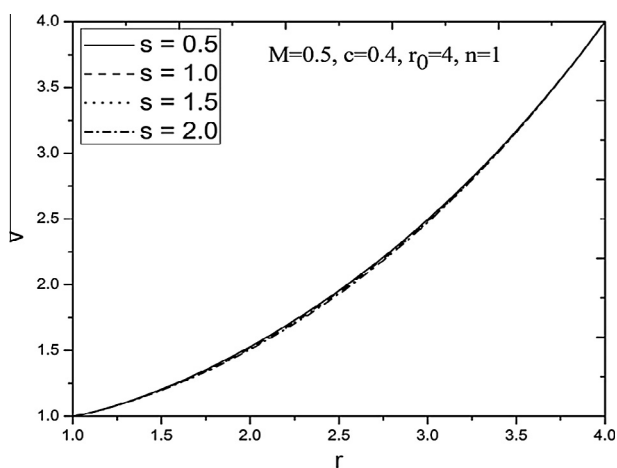


Figure 2a Effect of couple stress parameter on velocity distribution.

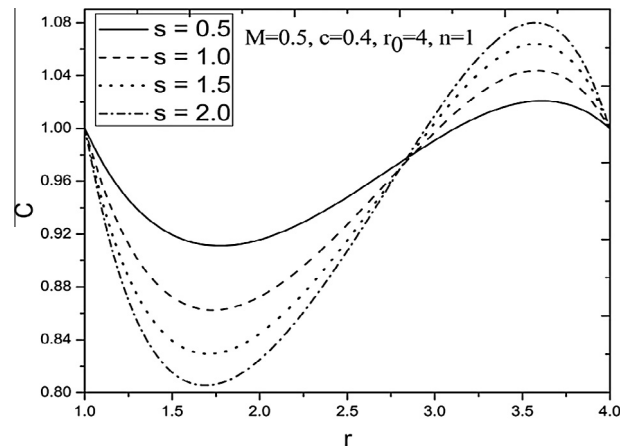


Figure 2b Effect of couple stress parameter on micro-rotation distribution.

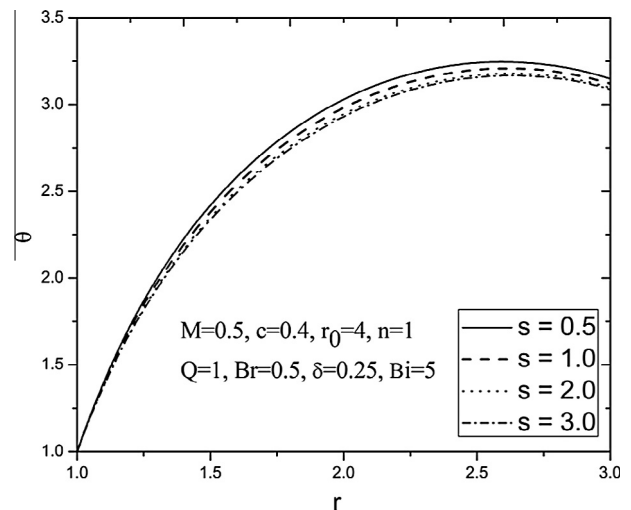


Figure 2c Effect of couple stress parameter on temperature distribution.

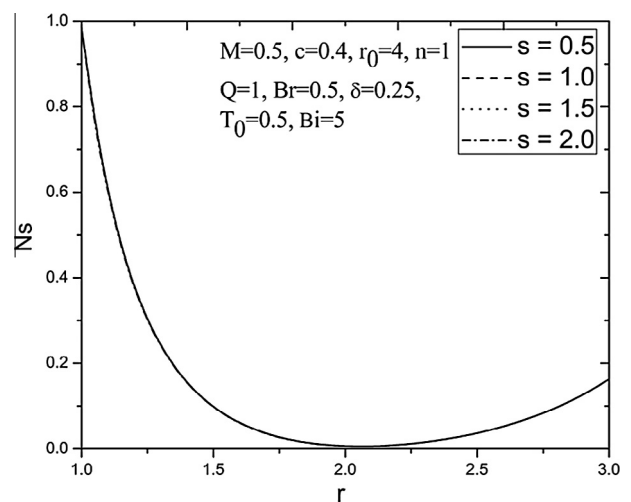


Figure 2d Effect of couple stress parameter on entropy generation number.

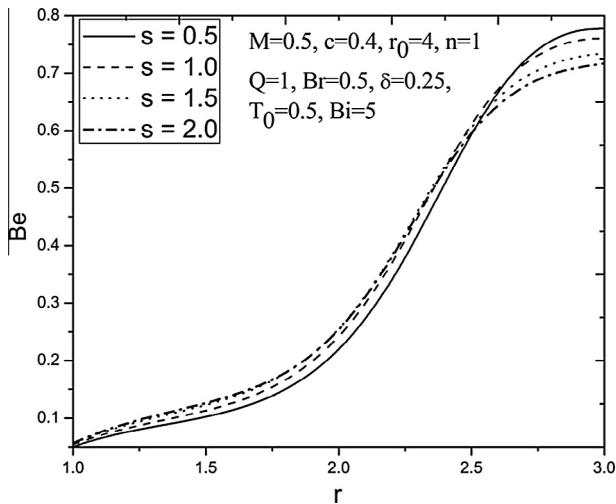


Figure 2e Effect of couple stress parameter on Bejan number.

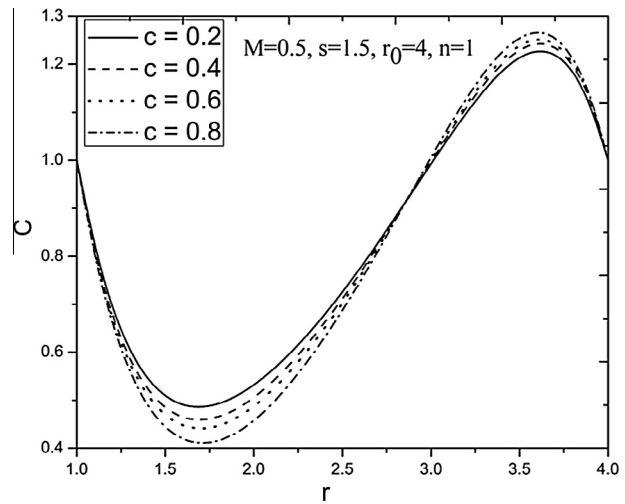


Figure 3b Effect of coupling number on micro-rotation distribution.

in the regime. This indicates that thermal energy is lowered in the regime and makes micropolar fluids attractive from the viewpoint of lubrication engineering, compared with conventional Newtonian viscous lubricants, an observation also consistent with other investigations, notably Gorla et al. [56] and Zueco et al. [57]. It is clear from Fig. 2d that there is no effect of s on Ns . The effect of couple stress parameter on Bejan number is displayed in Fig. 2e. As the couple stress parameter increases, Bejan number increases up to $r = 2.5$, whereas it clearly decreases towards the vicinity of the outer cylinder. In the definition of Ns and Be , viz Eqs. (17) and (20), there is an absence of the couple stress parameter, s . It is also absent in the temperature balance Eq. (9). The reduction in temperature with couple stress parameter indirectly therefore influences the Bejan number which is generally elevated. However, it does not markedly influence the overall local entropy generation rate, Ns (see Fig. 2d). Evidently larger Bejan numbers correspond to cooling of the flow regime. A similar trend has been reported by Makinde [58] also for non-Newtonian magnetic flows.

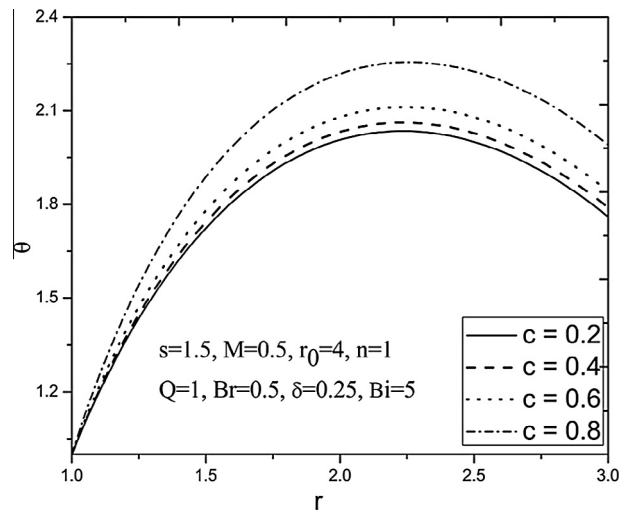


Figure 3c Effect of coupling number on temperature distribution.

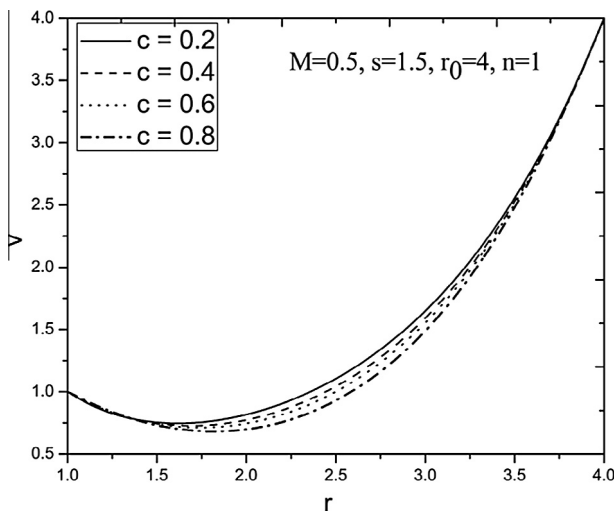


Figure 3a Effect of coupling number on velocity distribution.

Figs. 3a–3e display the influence of the coupling parameter (c) on the tangential velocity, microrotation, temperature, entropy generation distribution and Bejan distribution. The coupling parameter (c) characterizes the coupling of linear and rotational motion arising from the microrotation of the fluid molecules which is intimately associated with the translational momentum, as elaborated by Eringen [59]. Therefore the coupling parameter signifies the coupling between rotational viscosities and Newtonian dynamic viscosity. As $\kappa \rightarrow 0$, i.e., $c \rightarrow 0$, the micropolarity is absent and we retrieve the case of a Newtonian viscous fluid. It is apparent from Fig. 3a that the velocity profiles decrease with an increase of coupling parameter. Therefore, it can be concluded that the velocity in the case of micropolar fluid is less compared to that of viscous fluid. The deceleration in the flow is directly induced therefore by the presence of micropolar vortex viscosity which is absent within the framework of the Navier-Stokes (Newtonian viscous) model. Fig. 3b displays that an increase in cou-

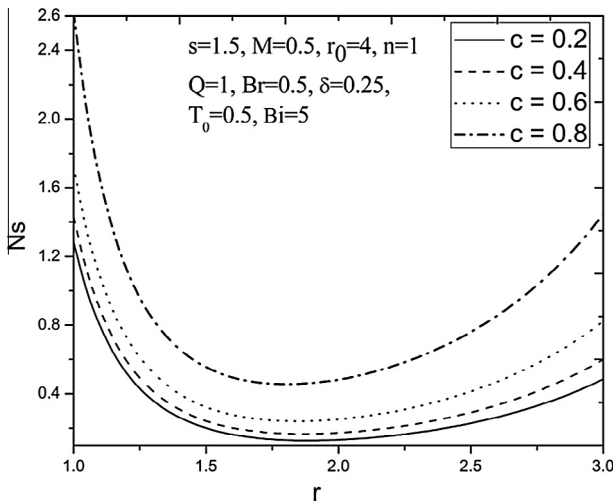


Figure 3d Effect of coupling number on entropy generation number.

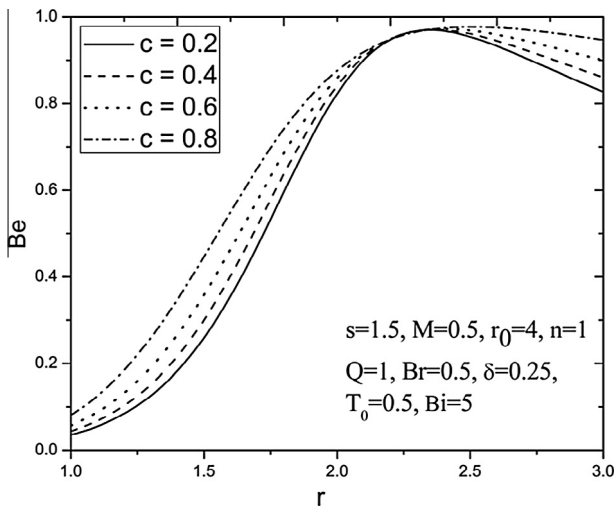


Figure 3e Effect of coupling number on Bejan number.

pling number initially decreases but thereafter strongly increases the microrotation magnitude. In other words greater vortex viscosity of the micropolar fluid encourages angular motions and so-called spin of the micro-elements only at larger distances from the incipience of motion (inner cylinder wall). Closer to the inner cylinder wall the rotary motions (spin) are inhibited, a feature which has also been reported by Gorla et al. [56] in curved body micropolar flows. Conversely the temperature is consistently elevated with an increase in coupling parameter. The regime is therefore heated by the presence of progressively stronger micropolar vortex viscosity. This pattern of behavior is consistent also with the computations of Nazar et al. [60]. It is clear from Fig. 3c that the peak temperature surfaces are at intermediate distances within the annular gap, i.e. far from either cylinder boundary. This is probably attributable to the convective cooling condition which serves to depress temperatures at the outer cylinder. Nevertheless the over-riding effect of coupling number is to energize the micropolar fluid and cause significant heating.

Fig. 3d displays the effect of coupling number (c) on the entropy generation distribution. As c increases entropy production increases throughout the annular gap; however, the effect is more pronounced in proximity to the inner cylinder. Since $\kappa \rightarrow 0$, i.e., $c \rightarrow 0$, represents the viscous fluid case, the entropy generation rate in the case of viscous fluids is substantially lower than that of the micropolar fluid case. This has significant implications in energy systems where strongly rheological fluids (e.g. micropolar) can be utilized to minimize entropy generation and thereby engineers can manipulate the effective thermal efficiency of such systems, as indicated by Assad [28,31]. Fig. 3e demonstrates that an increasing micropolar coupling parameter (c) serves to elevate the Bejan number gradually except in the region $2.2 < r < 2.5$. Bejan number tends to grow in magnitude from the inner cylinder steadily and peaks near the outer cylinder and thereafter, although the profiles begin to descend, they do markedly more gradually than rate of ascent prior to the peak.

In magneto-hydrodynamics, the relation between fluid flow field and magnetic field results in a transverse Lorentzian body force transverse to the line of application of the magnetic field, i.e. normal to the axial direction (it therefore acts in the tangential direction). Fig. 4a reveals that the tangential velocity values are decreased in the annulus region with an increasing Hartmann number (M). Increasing the values of Hartmann number (which is proportional to the axial magnetic field, B_0 , since $M^2 = \frac{\sigma B_0^2 a^2}{\kappa + \mu}$) enhances the Lorentzian magnetohydrodynamic drag force and this effectively decelerates the tangential flow. The axial magnetic field therefore provides a mechanism for controlling the tangential flow which is of interest in MHD energy systems, electromagnetic flow pumps and other industrial systems using electrically-conducting fluids as described by Cramer and Pai [61]. Fig. 4b displays the effect of Hartmann number on microrotation. An increase in Hartmann number results in initially suppressing the values of microrotation closer to the inner cylinder whereas further away towards the outer cylinder the trend is reversed and acceleration in angular velocity is observed. At weak magnetic field ($M = 0.1$) there is evidently very little influence on microrotation. The sensitivity of the microrotation field (C) to mag-

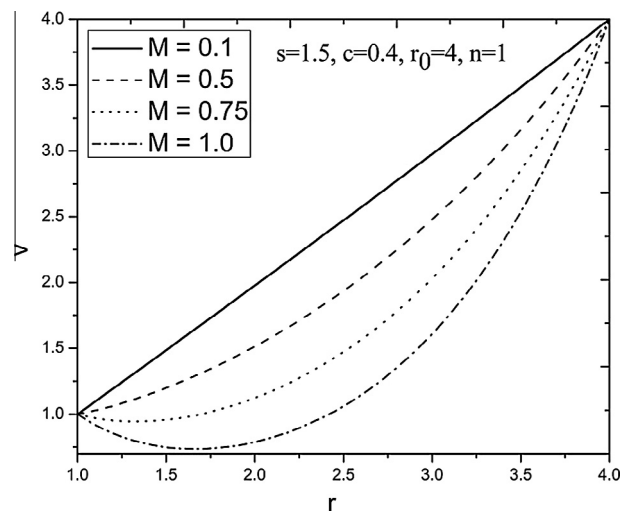


Figure 4a Effect of Hartmann number on velocity distribution.

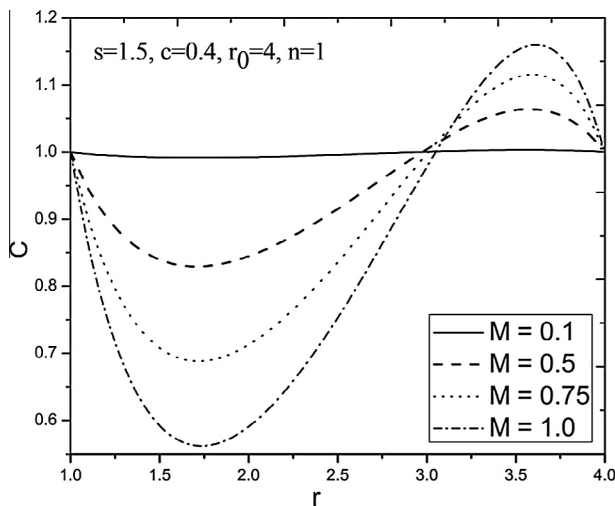


Figure 4b Effect of Hartmann number on microrotation distribution.

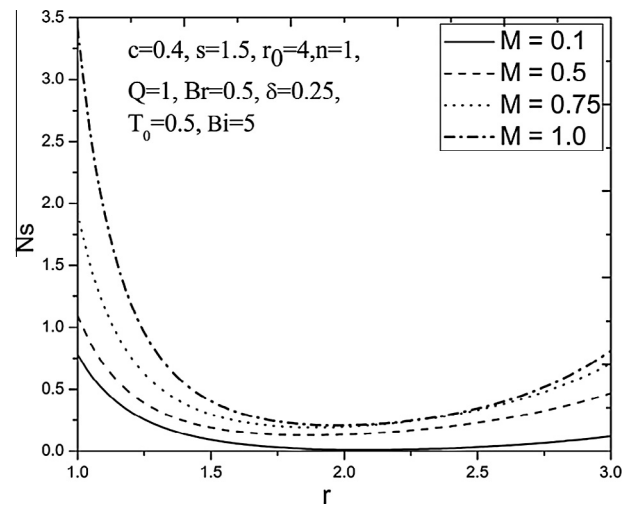


Figure 4d Effect of Hartmann number on entropy generation number.

netic field is inevitably attributable to the strong coupling of the tangential velocity and micro-rotation field equations. The Lorentzian magnetic body force only arises in the tangential flow momentum equation and not the micro-rotation equation. However, there are many terms in both equations featuring both v and C variables indicating that there is a strong inter-dependency of the tangential momentum and angular momentum fields. This enables the magnetic body force to influence the micro-rotation field. Therefore, while the axial magnetic field retards the tangential flow, it serves to have the opposite effect and enhances the angular velocity of micro-elements, i.e. micro-rotation not only when adequate space is provided for rotation of micro-elements. It is also interesting to note in Fig. 4a that the velocity profile for weak magnetic field ($M = 0.1$) evolves into an increasingly parabolic profile as M values increase. This observation has also been noted in many classical works on MHD including Shercliff [62]. We further note that when $M = 1.0$ there is an equivalence of the Lorentzian magnetic body force and the viscous

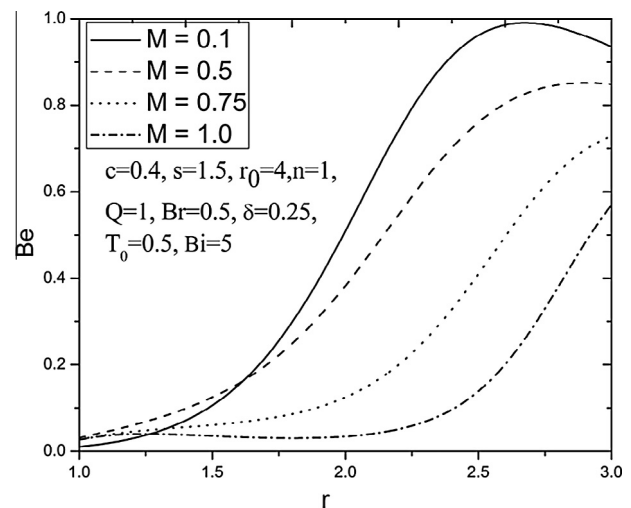


Figure 4e Effect of Hartmann number on Bejan number.

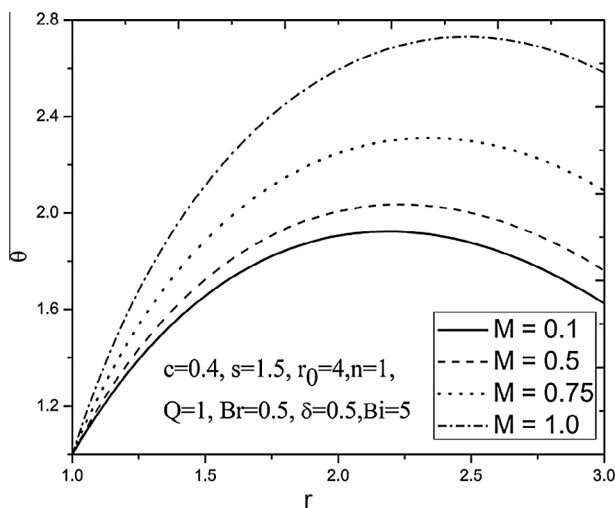


Figure 4c Effect of Hartmann number on temperature distribution.

hydrodynamic force in the regime. For $M < 1$, the viscous force dominates and vice versa for $M > 1$. Fig. 4c indicates that increasing Hartmann number (M) results in heating of the micropolar fluid, i.e. escalation in temperatures. Physically supplementary work must be expended by the micropolar fluid to drag it against the action of the magnetic field (inhibiting Lorentzian force). This generates kinetic energy which is dissipated as heat in the fluid. This is classical characteristic of the magnetohydrodynamic channel (and boundary layer) flows and has indeed been documented in many standard works in the field, including Cramer and Pai [61] and Shercliff [62]. The heating effect is observed to occur across the entire gap region. Fig. 4d demonstrates that as Hartmann number increases, the entropy generation number also increases. However, greater magnitudes are attained in the vicinity of the inner cylinder as compared to the outer cylinder and this is probably linked to the different thermal boundary conditions imposed at each cylinder wall. In comparison with the effects of other parameters (couple stress parameter and micropolar-

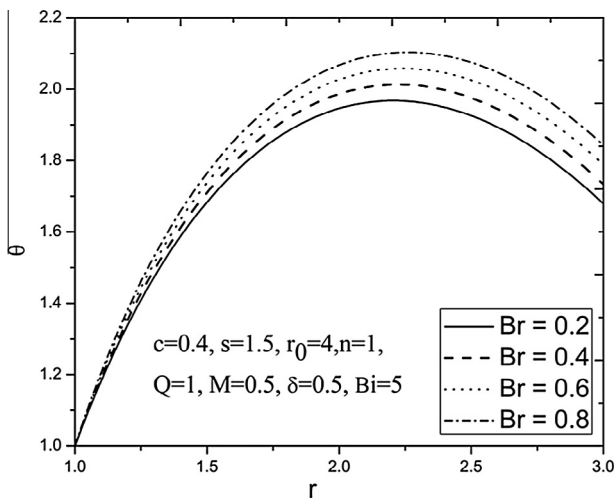


Figure 5a Effect of Brinkman number on temperature distribution.

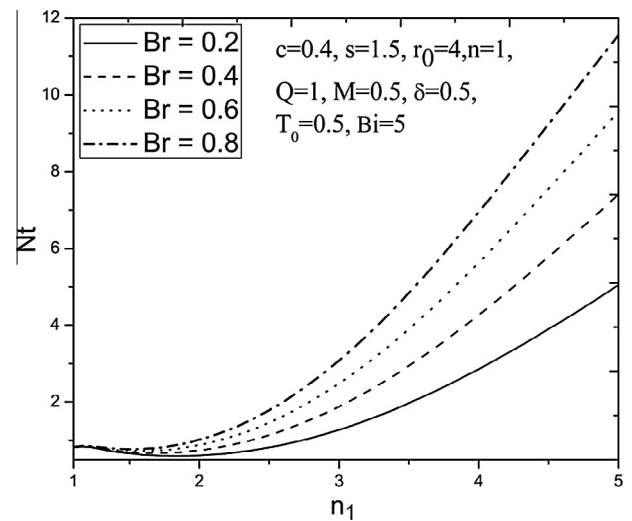


Figure 5d Effect of Brinkman number on total entropy generation number.

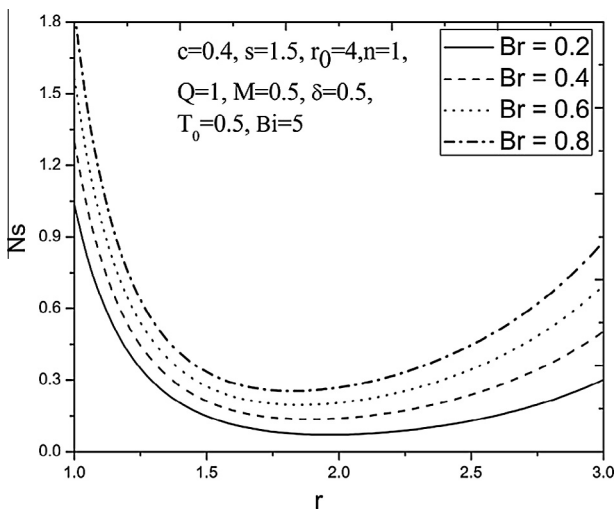


Figure 5b Effect of Brinkman number on entropy generation number.

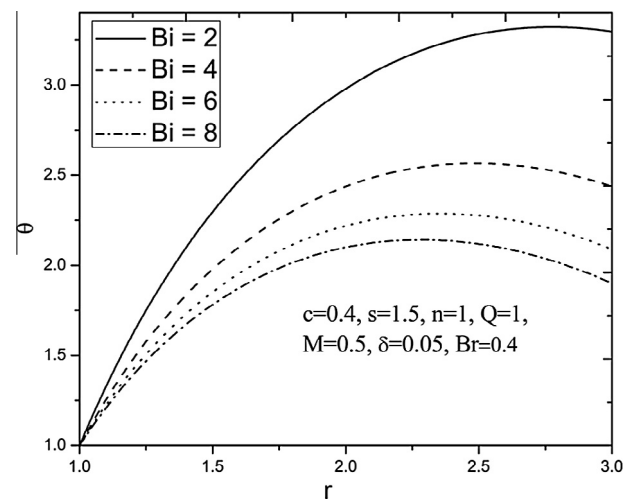


Figure 6a Effect of Biot number on temperature distribution.

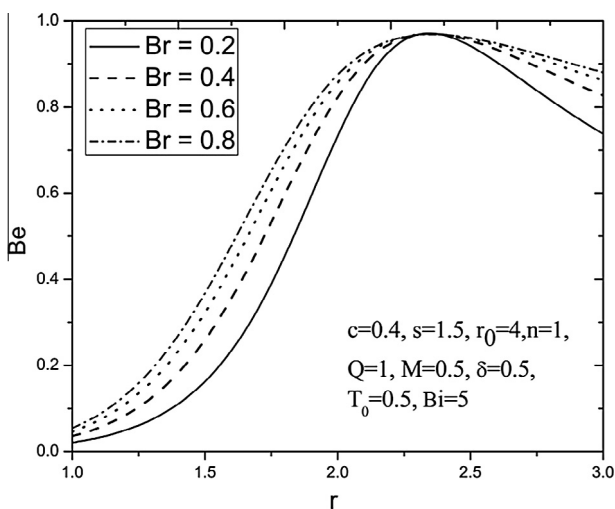


Figure 5c Effect of Brinkman number on Bejan number.

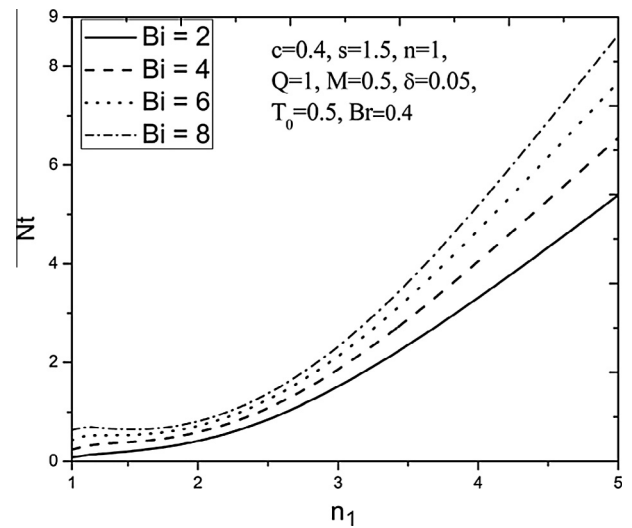


Figure 6b Effect of Biot number on total entropy generation rate.

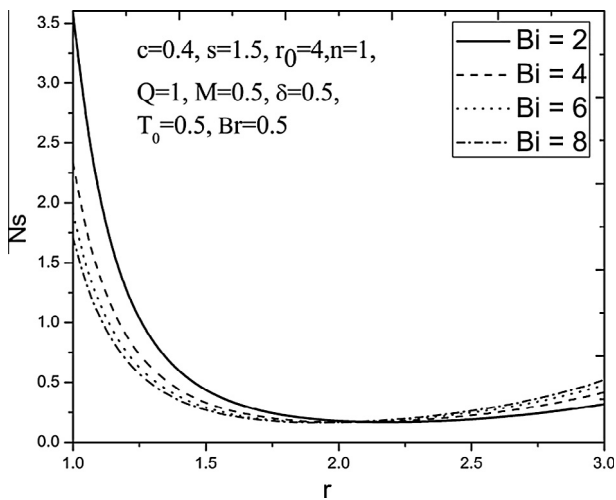


Figure 6c Effect of Biot number on entropy generation number.

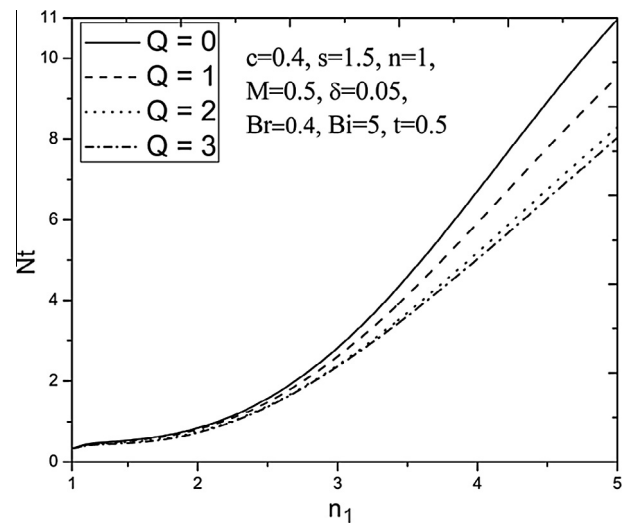


Figure 7b Effect of internal heat generation parameter on total entropy generation rate.

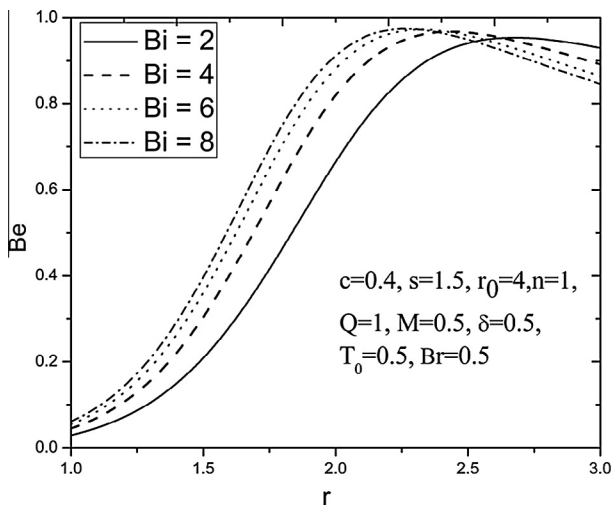


Figure 6d Effect of Biot number on Bejan number.

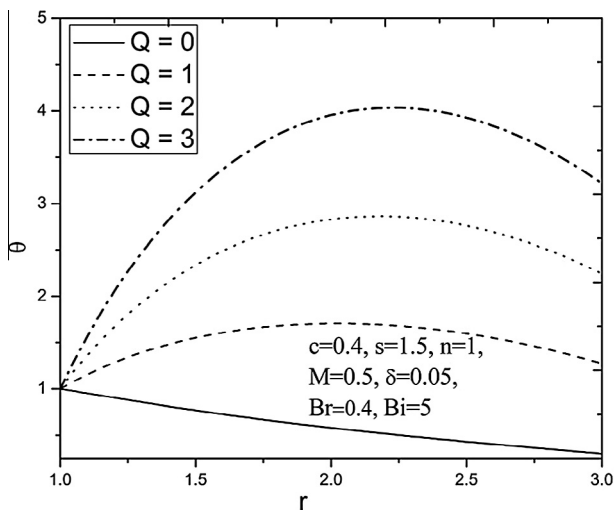


Figure 7a Effect of internal heat generation parameter on temperature.

ity), the impact of M on temperature and entropy generation rate is considerably greater, i.e. the magnetic field influences the temperature field more prominently than the rheological parameters do. This implies that the micropolar fluid microelements (particles) acquire more energy due to the magnetic effect and not due to friction effects at the wall. It is found from Fig. 4e that the Bejan number decreases gradually as we move towards the outer cylinder with an increase of magnetic parameter. Axial magnetic field, therefore results in the opposite effect on Bejan number compared with entropy generation rate. Internal fluid friction increases the Bejan number dramatically in the vicinity of the outer cylinder.

Brinkman number is a significant parameter in irreversibility analysis. The variation in temperature, entropy generation number, Bejan number and total entropy generation rate with respect to the Brinkman number (Br) is demonstrated in Figs. 5a–5d. Fig. 5a reveals that for $Br < 1$, with increasing Br from 0.2 to 0.8, the temperature increases entirely in the annulus region. The impact of the Brinkman number on non-dimensional entropy generation number is depicted in Fig. 5b. It is noticed that the Brinkman number enhances the entropy generation in the annulus region and these effects are more near the inner cylinder wall as compared to the outer cylinder wall. This may be due to the fact that near the inner cylinder the fluid temperature and velocity gradients are highest. Fig. 5c elucidates the effect of Br on Be . The Bejan number increases significantly with an increase in the Brinkman number. Effectively Br embodies the relative influence of heat produced by viscous dissipation and heat transported by molecular conduction. It therefore can be used to express the ratio of the viscous heat generation to external heating in thermofluid dynamics. Higher Br implies a lower contribution in thermal conduction generated via viscous dissipation and greater elevation in temperatures. Further, with the increase in radial distance (r) from the inner cylinder surface, Bejan number tends to 1 (approximately). This indicates that the irreversibility due to heat transfer dominates in this region. The Bejan number tends to zero near the inner cylinder surface. This indicates that the entropy (irreversibility) due to fluid friction dominates. It is found from Fig. 5d that as the Brinkman

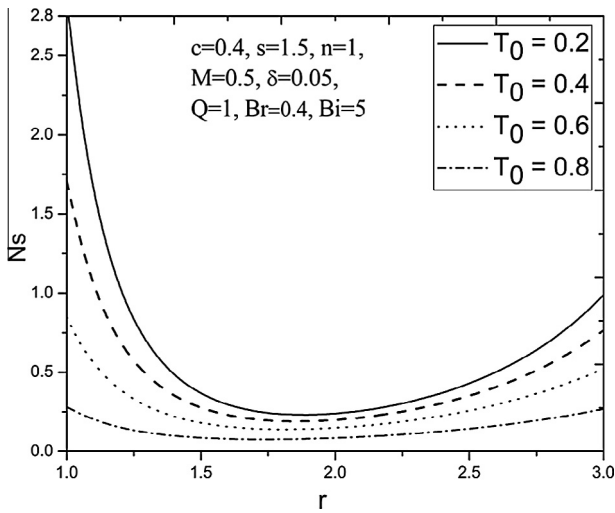


Figure 8a Effect of temperature ratio on entropy generation number.

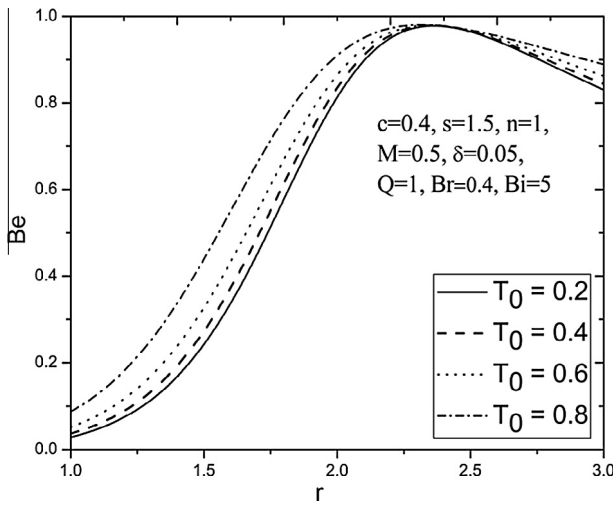


Figure 8b Effect of temperature ratio on Bejan number.

number increases, the total entropy generation profiles increase. These profiles have a similar trend; however, there is a variation in magnitudes.

Figs. 6a–6d portray the impact of the Biot number (Bi) on temperature and total entropy generation rate. It is found that as the Biot number increases, the temperature decreases in the entire annulus region of the channel. Greater Biot numbers, therefore generate cooling in the micropolar fluid regime. From Fig. 6b, it is clear that the total entropy generation rate increases with increasing the values of Biot number. Fig. 6c portrays the influence of the Biot number on N_s . As the Biot number increases, N_s decreases near the inner cylinder surface. The effect of the Biot number on Bejan number is displayed in Fig. 6d. It is evident that an elevation in Biot number increases the Bejan number gradually up to $r = 2.5$ and the opposite trend is observed in the region around the outer cylinder. Fig. 7a displays that an increase in internal heat generation (Q) results in higher fluid temperatures. The maximum temperature value is obtained at $r = 2.2$ (closer to the outer cylinder surface) as internal heat generation Q increases. Also, this figure demonstrates that the temperature profile is almost linear

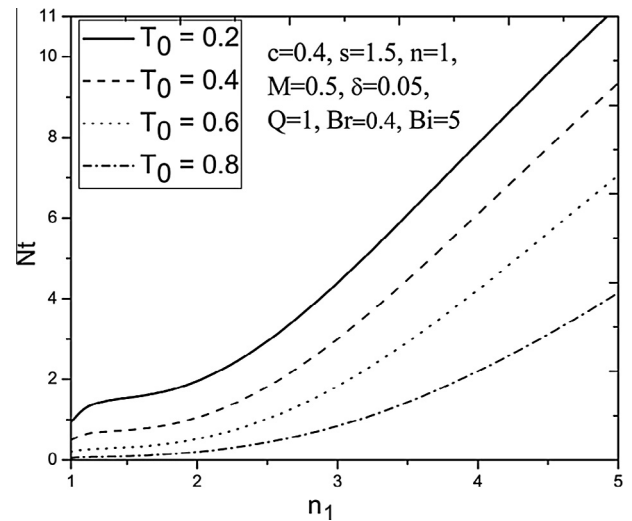


Figure 8c Effect of temperature ratio on total entropy generation rate.

in nature when the internal heat generation is zero ($Q = 0$). Moreover, the temperature profiles become increasing non-linear in nature as the internal heat generation increases. Fig. 7b shows that the total entropy generation decreases throughout the annulus region with an increase in the internal heat generation. The presence of a heat source is therefore assistive to a reduction in entropy generation, which is again of some interest in practical MHD energy systems. Figs. 8a–8c show the variation of the temperature ratio on entropy generation number, Bejan number and the total entropy generation rate. Fig. 8a clearly demonstrates the entropy generation decreases with an increase in the temperature ratio, $T_0 = \frac{T_\infty}{T_1}$ (which represents the ratio of the coolant fluid temperature to the inner cylinder surface temperature). It is clear from Fig. 8b that the temperature ratio enhances the Bejan number. Further, it is noticed that, as the temperature ratio increases, the total entropy generation rate gradually decreases in the entire annulus region shown in Fig. 8c. Therefore, as the regime is increasingly cooled, the global effect is to depress the entropy generation rate.

5. Conclusions

In the present work, a theoretical study of entropy generation in the steady-state flow of an incompressible, magneto-micropolar fluid in the annulus zone between co-rotating cylinders has been described. The non-dimensionalized linear momentum, angular momentum (micro-rotation) and energy conservation equations have been solved subject to physically appropriate boundary conditions. Exact closed-form expressions for velocity, microrotation and temperature, respectively, have been derived which are then utilized to obtain the entropy formulas. Validation of solutions with previous studies [63] has been conducted demonstrating close correlation. Numerical evaluation of the solutions has been depicted graphically and a systematic study was conducted to examine the influence of the emerging thermophysical, micropolar (non-Newtonian) and magnetic parameters on the key thermal and momentum characteristics. The key findings of this study are summarized as follows:

1. Increasing the couple stress effect in the micropolar fluid decreases the velocity and increases the microrotation and temperature.
2. An elevation in micropolarity parameter decreases the velocity in comparison with the viscous (Newtonian) fluid case.
3. For larger values of coupling (micropolar vortex viscosity) parameter, the velocity and microrotation of the fluid decrease whereas the temperature increases.
4. The entropy production is maximum near the inner rotating cylinder surface due to the high velocity and temperature gradients.
5. All the entropy profiles for different parameters show a maximum numerical value at the inner cylinder wall and they attain minimum values at the midpoint of the annulus region.
6. As the Hartmann (magnetic body force) number increases, the tangential flow is decelerated whereas the angular velocity (micro-rotation) and temperature magnitudes generally increase, i.e. the magnetic field causes resistance to the flow which results in decreasing the velocity and increasing the temperature.
7. The increasing values of Hartmann (magnetic) number manifest in an increase in the temperature as well as entropy generation number.
8. Total entropy generation rate increases with Brinkman number and internal heat generation, but the reverse trend is observed in the case when the temperature ratio increases.
9. Bejan number is enhanced with an increase in the temperature ratio (corresponding to higher coolant temperatures).
10. The total entropy generation rate is lowered with an increase in the internal heat generation parameter whereas micropolar fluid temperatures are elevated.
11. The total entropy generation is enhanced with a greater Brinkman number. Larger Biot number however leads to a decrease in temperature in the entire annulus region.
12. Generally, magnetic field and internal heat generation play a significant role within micropolar annular thermofluid systems and the impact of these parameters on entropy generation is quite significant. These effects therefore have a substantial influence in the design of MHD energy systems.

The present study is relevant to thermal optimization of electromagnetic flow processing and MHD energy systems using rheological working fluids. The present work has neglected magnetic induction effects which will be examined imminently.

Acknowledgement

We are grateful to the esteemed reviewers for their comments and suggestions which led to the improvement of the paper. The authors are very thankful to Prof. J. V. Ramana Murthy, NIT Warangal, for his valuable discussions.

References

- [1] D.M. Maron, S. Cohen, Hydrodynamics and heat/mass transfer near rotating surfaces, *Adv. Heat Transf.* 21 (1991) 141–183.
- [2] M. Couette, Studies relating to the friction of liquids, *Ann. Chim. Phys.* 21 (1890) 433.
- [3] K.J. Pillai, S.V.K. Varma, Flow of a conducting fluid between two co-axial rotating porous cylinders bounded by a permeable bed, *Indian J. Pure Appl. Math.* 20 (5) (1989) 526–536.
- [4] N.M. Bujurke, N.B. Naduvinamani, On the performance of narrow porous journal bearing lubricated with couple stress fluid, *Acta Mech.* 86 (1–4) (1991) 179–191.
- [5] Jaw-Ren Lin, Squeeze film characteristics of finite journal bearings: couple stress fluid model, *Tribol. Inter.* 31 (4) (1998) 201–207.
- [6] A. Ruggiero, A. Senatore, S. Ciortan, Partial journal bearings with couple stress fluids: an approximate closed-form solution, *Mech. Test. Diag.* 2 (2012) 21–26.
- [7] Schlichting, *Boundary Layer Theory*, McGraw-Hill, New York, 1968.
- [8] M.N. Channabasappa, K.G. Umapathy, I.V. Nayak, Effect of porous lining on the flow between two concentric rotating cylinders, *Proc. Indian Acad. Sci.* 88A (1979) 163–167.
- [9] D. Bathaiah, R. Venugopal, Effect of porous lining on the MHD flow between two concentric rotating cylinders under the influence of a uniform magnetic field, *Acta Mechanica* 44 (1982) 141–158.
- [10] T.S. Lee, Laminar fluid convection between concentric and eccentric heated horizontal rotating cylinders for low-Prandtl-number fluids, *Int. J. Numer. Method Fluids.* 14 (1992) 1037–1062.
- [11] R.L. Batra, B. Das, Flow of Casson fluid between two rotating cylinder, *Fluid Dyn. Res.* 9 (1992) 133–141.
- [12] R.L. Batra, M. Eissa, Helical flow of a Sutterby model fluid, *Polym.-Plast. Technol. Eng.* 33 (1994) 489–501.
- [13] J.C. Leong, F.C. Lai, Flow and heat transfer in concentric and eccentric rotating cylinders with a porous sleeve, in: *Proceedings of 8th AIAA/ASME Joint Ther. Phy. Heat Transf. Conf.*, 2002, pp. 24–26.
- [14] M.T. Ravanchi, M. Mirzazadeh, F. Rashidi, Flow of Giesekus viscoelastic fluid in a concentric annulus with inner cylinder rotation, *Int. J. Heat Fluid Flow* 28 (2007) 838–845.
- [15] M. Subotic, F.C. Lai, Flows between rotating cylinders with a porous lining, *ASME J. Heat Transf.* 130 (1-6) (2008) 102601.
- [16] A. Barletta, S. Lazzari, E. Magyari, I. Pop, Mixed convection with heating effects in a vertical porous annulus with a radially varying magnetic field, *Int. J. Heat Mass Transf.* 51 (2008) 5777–5784.
- [17] A. Mahmood, S. Parveen, A. Ara, N.A. Khan, Exact analytic solutions for the unsteady flow of a non-Newtonian fluid between two cylinders with fractional derivative model, *Commun. Nonlinear Sci. Numer. Simulat.* 14 (8) (2009) 3309–3319.
- [18] H.R. Mozayyeni, A.B. Rahimi, Mixed convection in a cylindrical annulus with rotating outer cylinder and constant magnetic field with an effect in the radial direction, *Scient. Iran.* 19 (1) (2012) 91–105.
- [19] A. Bejan, Second law analysis in heat transfer and thermal design, *Adv. Heat Transf.* 15 (1982) 1–58.
- [20] B.S. Yilbas, Entropy analysis of concentric annuli with rotating outer cylinder, *Exergy Int. J.* 1 (2001) 60–66.
- [21] S. Mahmud, R.A. Fraser, Second law analysis of heat transfer and fluid flow inside a cylindrical annular space, *Int. J. Exergy* 2 (4) (2002) 322–329.
- [22] S. Mahmud, R.A. Fraser, Analysis of entropy generation inside concentric cylindrical annuli with relative rotation, *Int. J. Therm. Sci.* 42 (5) (2003) 513–521.
- [23] M. Mirzazadeh, A. Shafaei, F. Rashidi, Entropy analysis for non-linear viscoelastic fluid in concentric rotating cylinders, *Int. J. Therm. Sci.* 47 (12) (2008) 1701–1711.
- [24] H. Hamakawa, H. Mori, M. Iino, M. Hori, M. Yamasaki, T. Setoguchi, Experimental study of heating fluid between two

- concentric cylinders with cavities, *Int. J. Therm. Sci.* 17 (2) (2008) 175–180.
- [25] M.S. Tshahla, O.D. Makinde, Analysis of entropy generation in a variable viscosity fluid flow between two concentric pipes with convective cooling at the surface, *Int. J. Phys. Sci.* 6 (25) (2011) 6053–6060.
- [26] S. Globe, Laminar steady state magneto hydrodynamic flow in an annular channel, *Phys. Fluids* 2 (1959) 404–407.
- [27] M. Kiyasatfar, N. Pourmahmoud, M.M. Golzan, I. Mirzaee, Thermal behavior and entropy generation rate analysis of a viscous flow in MHD micropumps, *J. Mech. Sci. Technol.* 26 (2012) 1949–1955.
- [28] M.E.H. Assad, Thermodynamic analysis of an irreversible MHD power plant, *Int. J. Energy Res.* 24 (2000) 865–875.
- [29] A.S. Butt, A. Ali, Entropy generation in MHD flow over a permeable stretching sheet embedded in a porous medium in the presence of viscous dissipation, *Int. J. Exergy* 13 (2013) 85–101.
- [30] M.El Haj Assad, Optimum performance of an irreversible MHD power plant, *Int. J. Exergy* 4 (1) (2007) 87–97.
- [31] M. El Haj Assad, C. Wu, Thermodynamic performance of an irreversible MHD power cycle running at constant Mach number, *Int. J. Ambient Energy* 29 (1) (2008) 10–20.
- [32] O. Mahian, S. Mahmud, I. Pop, Analysis of first and second laws of thermodynamics between two isothermal cylinders with relative rotation in the presence of MHD flow, *Int. J. Heat Mass Transf.* 55 (2012) 4808–4816.
- [33] O. Mahian, H. Oztop, I. Pop, S. Mahmud, S. Wongwises, Entropy generation between two vertical cylinders in the presence of MHD flow subjected to constant wall temperature, *Int. Commun. Heat Mass Transf.* 44 (2013) 87–92.
- [34] O. Mahian, S. Mahmud, S. Wongwises, Entropy generation between two rotating cylinders with magnetohydrodynamic flow using nanofluids, *AIAA J. Thermophys. Heat Transf.* 27 (1) (2013).
- [35] F. Selimefendigil, H.F. Öztop, MHD mixed convection and entropy generation of power law fluids a cavity with a partial heater under the effect of a rotating cylinder, *Int. J. Heat Mass Transf.* 98 (2016) 40–51.
- [36] F. Selimefendigil, H.F. Öztop, Influence of inclination angle of magnetic field on mixed convection of nanofluid flow over backward facing step and entropy generation, *Adv. Powder Technol.* 26 (2015) 1663–1675.
- [37] F. Selimefendigil, H.F. Öztop, MHD mixed convection of nanofluid filled partially heated triangular enclosure with a rotating adiabatic cylinder, *J. Taiwan Inst. Chem. Eng.* 45 (5) (2014) 2150–2162.
- [38] F. Selimefendigil, H.F. Öztop, N. Abu-Hamdeh, Natural convection and entropy generation in nanofluid filled entrapped trapezoidal cavities under the influence of magnetic field, *Entropy* 18 (2) (2016) 43.
- [39] S. Vimala, S. Damodaran, R. Sivakumar, T.V.S. Sekhar, The role of magnetic Reynolds number in MHD forced convection heat transfer, *Appl. Math. Model.* 40 (13–14) (2016) 6737–6753.
- [40] N. Freidoonimehr, S.S. Jafari, Second law of thermodynamics analysis of hydro-magnetic nanofluid slip flow over a stretching permeable surface, *J. Braz. Soc. Mech. Sci. Eng.* 37 (4) (2015) 1245–1256.
- [41] M.M. Rashidi, S. Bagheri, E. Momoniat, N. Freidoonimehr, Entropy analysis of convective MHD flow of third grade non-Newtonian fluid over a stretching sheet. *Ain Shams Eng J.* <http://dx.doi.org/10.1016/j.asej.2015.08.012> (Article in press).
- [42] M.M. Rashidi, S. Mahmud, N. Freidoonimehr, B. Rostami, Analysis of entropy generation in an MHD flow over a rotating porous disk with variable physical properties, *Int. J. Exergy* 16 (4) (2015) 481–503.
- [43] N. Freidoonimehr, M.M. Rashidi, S. Abelman, G. Lorenzini, Analytical modelling of MHD flow over a permeable rotating disk in the presence of Soret and Dufour effects: entropy analysis, *Entropy* 18 (5) (2016) 131.
- [44] A.C. Eringen, The theory of micropolar fluids, *J. Math. Mech.* 16 (1966) 1–18.
- [45] A.C. Eringen, Simple microfluids, *Int. J. Eng. Sci.* 2 (1964) 205–217.
- [46] A.C. Eringen, *Microcontinuum Field Theories. II: Fluent Media*, Springer-Verlag Press, New York, 2001.
- [47] V.K. Stokes, *Theories of Fluids with Microstructure*, Springer, New York, 1984.
- [48] G. Lukaszewicz, *Micropolar Fluids: Theory and Applications*, Birkhauser, Boston, 1999.
- [49] M. Reiner, The theory of plastic flow in the rotation viscometer, *J. Rheol.* 1 (1929) 5–10.
- [50] T. Ariman, A.S. Cakmak, L.R. Hill, Flow of micropolar fluids between two concentric cylinders, *Phys. Fluids* 10 (1967) 2545–2550.
- [51] H. Ramkissoon, S.R. Majumdar, Unsteady flow of a micropolar fluid between two concentric circular cylinders, *The Canadian J. Chem. Eng.* 55 (1977) 408–413.
- [52] F. Kamisli, Second law analysis of a disturbed flow in a thin slit with wall suction or injection, *Int. J. Heat Mass Transf.* 51 (2008) 3985–4001.
- [53] S. Mahmud, R.A. Fraser, The second law analysis in fundamental convective heat transfer problems, *Int. J. Therm. Sci.* 42 (2003) 177–186.
- [54] D. Srinivasacharya, K. Hima Bindu, Entropy generation in a porous annulus due to micropolar fluid flow with slip and convective boundary conditions, *Energy* 111 (2016) 165–177.
- [55] J. Srinivas, J.V. Ramana Murthy, Second law analysis of the flow of two immiscible micropolar fluids between two porous beds, *J. Eng. Thermophys.* 25 (1) (2016) 126–142.
- [56] R.S.R. Gorla, W.R. Schoren, H.S. Takhar, Natural convection boundary layer flow of a micropolar fluid over an isothermal cone, *Acta Mech.* 61 (1986) 139–152.
- [57] J. Zueco, O. Anwar Bég, H.S. Takhar, Network numerical analysis of magneto-micropolar convection through a vertical circular non-Darcian porous medium conduit, *Comput. Mater. Sci.* 46 (2009) 1028–1037.
- [58] O.D. Makinde, Entropy analysis for MHD boundary layer flow and heat transfer over a flat plate with a convective surface boundary condition, *Int. J. Exergy* 10 (2) (2012) 142–154.
- [59] A.C. Eringen, *Theory of micropolar fluids*, Technical Report, School of Aeronautics and Astronautics, Purdue University, Indiana, USA, July, 1965.
- [60] R. Nazar, N. Amin, I. Pop, Mixed convection boundary layer flow from a horizontal circular cylinder in micropolar fluids: case of constant wall temperature, *Int. J. Numer. Meth. Heat Fluid Flow* 13 (2003) 86–109.
- [61] K.C. Cramer, S.I. Pai, *Magneto-fluid Dynamics for Engineers and Applied Physicists*, MacGraw-Hill, New York, 1973.
- [62] J.A. Shercliff, *A Textbook of Magnetohydrodynamics*, Cambridge University Press, UK, 1965.
- [63] M.E.H. Assad, H.F. Öztop, Parametric study of entropy generation in a fluid with internal heat generation between two rotating cylinders subjected to convective cooling at the surface, *ISRN Chem. Eng.* (2012) 9 941587.